Tropical Storm Kyle (2002) and Cold-Air Damming: Their Interactions and Impacts on Heavy Rainfall in the Carolinas

Jose M. Garcia-Rivera[1,4], Yuh-Lang Lin[1,2,@]

and

Yevgenii Rastigejev[1,3]

[1]Department of Energy & Environmental Systems

[2]Department of Physics

and

[3]Department of Mathematics

North Carolina A&T State University

[4]I.M. Systems Group

Reference: Garcia-Rivera, J., Y.-L. Lin, and Y. Rastigejev, 2015: Interactions of Tropical Storm Kyle (2002) and Cold-Air Damming and Their Impacts on Heavy Rainfall in the Carolinas. Meteorology and Atmospheric Physics (MAAP, DOI 10.1007/s00703-015-0421-1, Online First)

The final publication is available at link.springer.com

[@]Corresponding author address: Dr. Yuh-Lang Lin, 302H Gibbs Hall, North Carolina A&T State University, 1601 E. Market Street, Greensboro, NC 27411. Email: ylin@ncat.edu

Abstract

The interactions between an Appalachian cold-air damming event and the near-passage of Tropical Storm Kyle (2002) along the coastal Carolinas are assessed by using a numerical weather prediction model. As the storm moved along the coastline, it began extra-tropical transition, bringing heavy rains to both the coastal region and inland towards the Piedmont of North Carolina. Our goal is to quantify the effects of both interacting weather systems on heavy precipitation in order to improve the dynamical understanding of such effects, as well as precipitation forecasts in the study region. A series of sensitivity tests were performed to isolate and quantify the effects of both systems on the total accumulated precipitation. It was found that (a) for this type of along-coast track, the pre-existing cold-air damming played only a minor role on the total accumulated precipitation, (b) the outer circulation of Kyle weakened the cold-air damming due to a redirection of the mean flow away from the east side of the Appalachian Mountains, and (c) the combination of Kyle with a shortwave mid to upper-level trough and a surface coastal front were responsible for the heavy precipitation experienced in the study area through the advection of moisture, vorticity, and the forcing of upward motion.

1. **Introduction**

The phenomenon known as cold-air damming (CAD) consists of a “trapping” of cold air mass against a mountain range, with effects ranging from persistent low-level cloudiness to stratiform precipitation (Richwien 1980). A CAD signature is commonly seen whenever higher sea-level pressures (SLPs) and lower near-surface temperatures are observed just east of the Appalachian Mountains, with lower and higher values of the respective fields at each side and to the southwest (see Bell and Bosart 1988). Numerous studies have been conducted to understand the dynamics of CAD events over the past few decades from a range of different approaches (Richwien 1980; Forbes et al. 1987; Stauffer and Warner 1987; Bell and Bosart 1988; Xu 1990; Xu and Gao 1995; Bailey et al. 2003). CAD is especially noticeable in the southern Appalachian Mountains, which is our study region, but it can occur in the northern slopes of Alaska, eastern Rockies, southern Alps and the Sierra Madre Oriental of Mexico, among other regions. Southern Appalachian CAD has historically posed challenges for weather forecasting along the eastern slopes of the mountains (Richwien 1980; Stauffner and Warner 1987; Xu and Gao 1995; Lackmann 2011, and references therein). Although CADs occur more often in winter, they can occur during most of the year if the given necessary conditions are met. In fact, a climatology study of CAD events in the southern Appalachians by Bailey et al. (2003; hereafter B03) revealed that the majority of the events were detected during the month of September (see their Figure 5).

Recently, several studies have analyzed and detected CADs and their interactions with passing tropical cyclones (TCs) near the southern Appalachians. For example, Srock and Bosart (2009; hereafter SB09) conducted a case study of a TC-induced CAD event with Tropical Storm Marcos (1990). Their analysis showed that Marcos forced the development of two separate CAD-coastal front events as it approached the southern Appalachians from the south, after landfall in the Florida

Panhandle. Damaging flooding due to heavy precipitation along the coasts of Georgia and the Carolinas occurred during this case. It was argued in SB09 that the CAD was crucial in producing the heavy precipitation through the forcing of ascending air near the coastal front and moisture advection. Our case setup differs from SB09 in that it consists of: 1) A weak tropical storm moving along the coasts of Georgia and the Carolinas, while undergoing extra-tropical (ET) transition, and 2) A pre-existing CAD east of the southern Appalachians prior to storm passage.

More recently, renewed interest can be found among operational weather forecasters in National Weather Service WFOs within the Eastern and Southern regions about the role of TCs interacting with CAD events near the southern Appalachians (Smith et al. 2013). This is due to the lack of understanding of the role of TC-CAD interactions on heavy precipitation that could produce flash flooding along the Piedmont region from the Carolinas to Georgia. It is based on this interest that we pursue our study. A series of sensitivity tests will be run with a full-physics mesoscale model to shed light on how a combination of a coastal TC track and a CAD event can influence precipitation or not.

Our study is concentrated on the Appalachian Damming Region (ADR) and coastal region from Georgia (GA) to North Carolina (NC). The ADR is defined here as the region extending from the foothills on the eastern slopes of the Southern Appalachian Mountains to the Piedmont region of South Carolina (SC), NC and Virginia (VA), bordered to the west by the Appalachian Mountains and to the east by the coastal plains. This region has been known to have difficult weather forecasting problems associated with CADs in the past (e.g., Bell and Bosart 1988, and references therein), therefore making the CAD during the passage of transitioning Tropical Storm Kyle (Kyle hereafter) an interesting case to analyze.

In this study, we propose that the effect of CAD on precipitation associated with the passage of a TC along the coastal Carolinas is minor. The transitioning TC in combination with a mid-to upper-level trough and surface coastal front are said to be the main drivers of all heavy precipitation amounts accumulated in our study region. This paper is organized as follows: An overview of Kyle will be presented in Section 2. The numerical model and experimental design are described in Section 3. An observational verification by using two reanalysis datasets is shown in Section 4. The simulated tracks are compared in Section 5. In addition, CAD detection and a detailed assessment of each of the simulations are presented. In Section 6, the impacts of the interaction of CAD and Kyle on precipitation are discussed. Finally, a summary and concluding remarks of our study are presented in Section 7.

2. **Synopsis of Tropical Storm Kyle (2002) and the existence of CAD**

Kyle was a long-lived tropical cyclone that developed far-east of Bermuda by 20 September and became ET while tracking along the NC coastline on 12 October (Stewart 2002). The system had a non-tropical origin and tracked, erratically at times, in a general westward course until reaching the United States coastline in SC by 11 October. It became a hurricane (peak 39 m s^{-1} or 75 kts) while over open waters of the Atlantic Ocean in 26-28 September.

Our focus period is from 0000 UTC 10 October to 0000 UTC 13 October (10/10/00Z – 10/13/00Z hereafter), a total of 3 days. At the beginning of this period the system was a tropical depression with surface winds of 13 m s^{-1} (25 kts) east of Florida (FL), moving westward and beginning a poleward re-curvature by the end of 10/10, tracking in response to an approaching shortwave trough from the west. Meanwhile, the isobars depicted a CAD signature in the ADR, while a stationary front was marked just offshore the Carolina coast in the NOAA-WPC surface analysis (not shown). During 10/11, the system moved roughly parallel and near the FL-GA coastline, eventually making landfall in SC in the afternoon at around 17Z as a minimal intensity tropical storm with sustained winds of 18 m s^{-1} (35 kts). A second landfall with the same intensity occurred at 22Z. While moving along the NC coastline in 10/12, the system strengthened slightly to 21 m s^{-1} (40 kts) before losing its tropical characteristics at around 18Z on the same day, while reportedly merging with a frontal system (Stewart 2002). By that point, Kyle and its remnants were offshore and moving away from the NC Outer Banks.

A CAD was present during Kyle's approach and passage east of the ADR during the period of 10/11-10/12 (Figs. 1-5). This was evidenced by surface maps and observations available at the NOAA Weather Prediction Center (WPC 2014a). Smith et al. (2013) provided additional observational evidence in supporting the occurrence of CAD while Kyle was near. The fact that there was a TC-CAD interaction occurring during this period made it a good case for analysis. A significant amount of storm-total precipitation was recorded across central NC with a peak total of 220 mm of rainfall in Butner (WPC 2014b). It is unclear if the large amount of rainfall in the ADR during Kyle's passage was due to the interaction of Kyle and the CAD. Our main goal in this paper is to isolate the influences of the storm and CAD separately.

3. **Numerical Model Description and Experimental Design**

Three numerical experiments have been performed in this study, which are described in the following and summarized in Table 1.

The Weather Research and Forecast (WRF-ARW) model version 3.4 was used to simulate the CAD event in the ADR during Kyle's passage along the Carolina coast. Additional WRF-ARW details can be found in Skamarock et al. (2008). The simulations were set with a single domain with a horizontal grid spacing of 9 km (250 X 250 grid intervals) centered on the ADR in western NC. They were set with 48 hyperbolic-eta vertical levels and the initial time conditions were 10/10/00Z, when the Kyle was east of FL as a tropical depression with winds of 13 m s^{-1} (25 kts). This particular choice was made looking for a far-enough distance of the storm from any influence in the ADR at initial conditions. The model output frequency was set to 60 minutes, ending at 10/13/00Z while the storm had transitioned into an ET cyclone offshore NC and moving eastward. The ERA-Interim 0.7° by 0.7 ° (~ 77 km) global reanalysis dataset (Dee et al. 2011) was used to initialize the model. The selected microphysics parameterization scheme was the WSM 6-class scheme (Hong and Lim 2006). The planetary boundary layer (PBL) scheme used was the Yonsei University PBL (Hong et al. 2006). The Kain-Fritsch cumulus parameterization scheme was used for the single domain in all simulations. The selected shortwave (SW) radiation scheme was the Goddard scheme and the longwave (LW) radiation scheme was the Rapid Radiative Transfer Model (RRTM), based on Mlawer et al. (1997). Also, the update of sea surface temperature (SST-update) was turned on for the simulation at each time step.

3.1 ***Control (CTL) case***

The control case (CTL hereafter) was performed to replicate the atmospheric environmental conditions that occurred in the study region for the period of 10/10/00Z-10/13/00Z. The configuration described above should allow account of the factors that may have contributed to heavy precipitation in this event. Those were: Kyle, the CAD, the coastal front (CF hereafter), the shortwave trough, and the topographic conditions that characterize our study region.

3.2 ***No-storm (NS) case***

A case identical to CTL except with Kyle removed (NS hereafter) was performed to investigate the impacts of the TC on precipitation. A bogus vortex scheme (Xiao et al. 2000; Fredrick et al.

2009) available in the model package was introduced in order to remove Kyle from the initial conditions of this particular simulation. Such scheme not only works to introduce, but also has an option to remove vortices at the initial time step. In addition, all surface fluxes of heat and moisture were deactivated throughout the simulation period to effectively dissipate the storm (effects on precipitation discussed in Section 6.1). This combination of bogus vortex removal and removal of fluxes worked well in removing Kyle from the simulation. The details are discussed in the next section.

*3.3 **No-mountain (FLAT) case***

Another case identical to CTL except with the topography removed (FLAT hereafter) was performed to investigate the CAD effects on precipitation. The land-ocean distribution remained unchanged but all the land area had a constant height of 0 m.

*3.4 **Additional datasets***

Two reanalysis and one observational datasets were utilized to verify the simulation results. The first reanalysis dataset is the aforementioned ERA-Interim (ERA-I) global analysis and the other is the North American Regional Reanalysis (NARR; Mesinger et al. 2006), which has a horizontal resolution of 32 km. The latter has the advantage of depicting convective precipitation, which is useful in tracking the heaviest rainfall areas. The CPC .25 º x.25 º (~ 27.5 km) Daily US Unified Gauge-Based Analysis of Precipitation (CPC Precipitation, hereafter; data provided by the NOAA/OAR/ESRL PSD, Boulder, Colorado, USA, from their Web site at http://www.esrl.noaa.gov/psd/). The latter was used to verify the observed accumulated event precipitation. These tools served to assess the quality of the simulations.

4. **Observational data analysis of the event**

A comparison of the ERA-I and NARR reanalysis datasets was performed to verify our simulation results. These two data sources were used to analyze surface fields that would show the CAD event and the TC as it tracked along the coastline.

4.1 ***ERA-I analysis***

The SLP, 10-m winds and 2-m temperature were used for the ERA-I data in a 12-hourly temporal resolution during 10/10/00Z-10/12/12Z (Figs. 1-2). At the initial time step, the isobars depicted the location of Kyle as a weak low pressure near Abaco Island (Fig. 1a). Also, a strong high pressure system that was located over New England provided for the characteristic northeasterly flow east of the Appalachians that resulted in a CAD. The lower temperatures concentrated east of the mountains gave further proof that a CAD was present at that moment. Further west, a weak surface low was developing in the Lower Mississippi Valley. All of these were the main surface features that stood out in the initial conditions.

By 10/10/12Z, the CAD was present in the ADR, while Kyle was located near the FL east coast (Fig. 1b). A west-northwesterly track of the storm ensued as it was just east of Cape Canaveral by 10/11/00Z (Fig. 1c). It is worth noting here that the ERA-I solution brought the storm closer to FL than in the best track and our simulations (see Fig. 6). The CAD remained well-defined both in the in both pressure and thermodynamic fields, while Kyle began a poleward re-curvature as it accelerated in response to an approaching mid to upper-level trough. By 10/11/12Z, the storm was near the GA-SC border coastline with a CAD still present (Fig. 1d). As Kyle began to recurve and strengthen, likely due to increased barcolinicity as it merged with a CF. Kyle began to lose its tropical characteristics as it moved over eastern NC by 10/12/00Z, while still strengthening (Fig. 2a). In addition, a substantial increase of baroclinicity, as depicted by the strong horizontal temperature gradient, was associated with the low. More importantly, the CAD signature was no longer present at this time due to the advection of winds from the northwest, away from the mountains. By 10/12/12Z, the low associated with Kyle was offshore Cape Hatteras and moving away as an intensifying post-tropical cyclone (Fig. 2b).

4.2 NARR analysis

NARR data was also used to test the consistency of the ERA-I and simulation results. Using SLP, 2-m potential temperature (θ) and 10-m winds, an examination to the total and convective precipitation accumulations was also done for the same time period as with ERA-I (Figs. 3-5). As with ERA-I, at 10/10/00Z the weak Kyle was located near Abaco Island, a strong surface ridge was over New England, and a CAD signature was evident in the ADR both in the isobars and colder θ values there (Fig. 3a). Between 10/10/00Z and 10/11/12Z the storm approached the Carolina coastline while showing signs of strengthening (Fig. 3c; Figs 4a and c). Simultaneously, non-convective precipitation began to accumulate in the study region beginning at 10/10/12Z, with significant increases (including convective form) during 10/11 as Kyle closed in (Figs. 3b and d; Figs 4b and d). A well-defined CAD signature was present until 10/11/00Z, later beginning to weaken as the storm approached the ADR. Kyle began to re-strengthen and accelerate northeastward along the Carolina coastline by 10/11/12Z (Fig. 4c). The CAD signature became weaker, as opposed to ERA-I during the same time. The discrepancies seem to be in the strength and track timing of Kyle, with NARR showing a deeper low (i.e. stronger influence on CAD erosion) and associated surface circulation, while ERA-I had a weaker system. In addition, Kyle was tracking at a slightly slower speed in the NARR data, which was closer to the best-track positions (Stewart 2002). By 10/12/00Z the low was centered just to the west of Cape Fear with no CAD signature (Fig. 5a). Meanwhile, at 10/12/00Z the heaviest convective precipitation was concentrated in the coastal plains of both Carolinas (Fig. 5b). At the end of this period, a post-tropical low stands out offshore Cape Hatteras (10/12/12Z; Fig 5c). As with ERA-I, NARR's Kyle strengthened as it became post-tropical, while convective precipitation had accumulated in eastern NC and parts of SC, the latter associated with the cold front that extended through the region at that point (Fig. 5d).

Despite the minor discrepancies in Kyle's track, intensity, and the strength of the CAD event, both ERA-I and NARR effectively represented the CAD and transitioning TC observed in this case study. In addition, the two datasets confirmed that there was a pre-existing CAD in the ADR as Kyle approached the area. It was also observed that the CAD eroded as the storm's circulation moved in the vicinity of the ADR, effectively ending as the mean surface flow shifted from the northwest in that region.

5. **Verification of simulated storm tracks and CAD detection and assessment**

*5.1 **Verification of simulated storm tracks***

Figure 6 shows the simulated tracks in CTL and FLAT, respectively, compared to the observed track based on the National Hurricane Center report (Stewart 2002). The simulated storm in CTL (dotted line in Fig. 6a) shows that there was an overall agreement both in storm track and moving speed, thus making it a realistic simulation of Kyle. The recurving to the northeast is well captured by the model despite a slight leftward bias of the track. Interestingly, the resultant simulated track in FLAT (Fig. 6b) was remarkably similar to its counterpart in CTL. This indicates that there was little to no effect of the mountains and CAD on Kyle's track and motion, which was anticipated and confirmed by the sensitivity test FLAT. In summary, the storm track in these two simulations containing Kyle was consistent with the observed track, thus giving confidence for further analysis of this case.

5.2 ***Simulation intercomparison: CAD detection and TC-CAD interactions***

The left panels of Figs. 7-15 depict overlays of SLP, θ, and 10-m winds (in 12-hourly intervals), while the right panels contain vertical cross-sections of θ and horizontal wind barbs. These fields depicted the simulated TC-CAD interactions in this case, additionally confirming the existence of a CF (similar to that found in SB09). This finding represents a strong pre-existing baroclinic zone that presumably aided Kyle on its ET transition as it passed near the ADR.

5.2.1 ***CTL simulation***

At initial conditions (10/10/00Z) the location and strength of Kyle (tropical depression) agreed with NARR, ERA-I and NHC best track datasets (Fig. 7a). It was located near Abaco Island while a well-defined CAD signature was present in the ADR. The lower θ values east of the Appalachians were collocated with the isobars and the northeasterly wind flow. The CF can be seen along the GA-NC coastline with a well-defined horizontal temperature gradient. The 10/10/00Z cross-section also revealed the CAD, with the colder air-mass trapped in the east of the mountains (Fig. 7b) and surface east-northeasterly to northeast flow in the ADR. The CF was also visible at this particular cross-section (along 35°N). By 10/10/12Z Kyle was near Cape Canaveral while the CAD and CF features persisted (Fig. 7c). As the storm moved westward the wind direction near the GA-NC coastline turned easterly, thus enhancing the frontal boundary through advection of the warm and humid air-mass (confirmed by the wind barbs turning from southeast in the coast to northeast inland in Fig. 7d). The cold air-mass had become better-defined (Fig. 7d), thus depicting a slight intensification of the CAD (favored by the stronger ridge over New England).

Temperatures in the study region increased as Kyle approached the GA coastline at 10/11/00Z due to a more predominant southeasterly flow that brought warm-air advection (Fig. 8a). However, the CAD was still present, albeit not as strong as 12 h earlier. The position of the CF shifted further inland, as evidenced by the wind vectors and temperature gradients in Figs. 8a and 8b. The CAD signature became zonally narrower as Kyle continued approaching the ADR, as shown by the "wedging" limited to the western NC Piedmont and Foothills. The setup changed little as Kyle moved over the GA coast at 10/11/12Z (Fig. 8c). Likewise, the cross-section confirmed the continuity of the CAD despite its limited zonal distribution (Fig. 8d). In fact, the front had displaced further west, now abeam the western Piedmont and close to the Foothills as the southeasterly flow prevailed at the east of the study region (Figs. 8c and 8d). Until this point, all indicators confirmed that a CAD was still occurring within the ADR.

As Kyle moved along the SC-NC coastline it began its ET transition, as revealed by the increased baroclinicity near its center by 10/12/00Z (Fig. 9a). During transition the low intensified until the end of the study period. Meanwhile, the CAD signature was no longer present in the isobars. ADR mean wind flow regime shifted from the north, which helped to erode the damming as it began to advect the air mass away from the mountains. At the same time the front had retrograded eastward in response to the influence of the storm, and the colder air-mass in the ADR moved eastward in the wake of the transitioning storm (Fig. 9b). By 10/12/12Z Kyle was displaying a thermodynamically-baroclinic structure, with a cold front off the NC-SC coastline and a warm front extending from the storm into the Atlantic Ocean (Fig. 9c). This is consistent with NHC best track data indicating transition during this same period. The CAD had already ended, and cold-air advection predominated in the ADR as a northwesterly wind flow established in the western side of ex-Kyle. By then, the colder air-mass spread throughout the ADR and coastal regions (Fig. 9d).

An examination of the surface fields and cross-sections confirmed the track of Kyle along the GA-NC coastal region as it began ET transition, while a pre-existing CAD event was present in the ADR. The existence of a CF that first moved inland and then retreated back to the coast in response to the storm's influence was also observed (discussed in Sec. 6.2).

5.2.2 ***NS simulation***

As with case CTL (Figs. 7-9), a similar analysis of fields in NS verified the removal of the storm from the domain (Figs. 10-12). At 10/10/00Z the pressure and wind-fields confirmed that the circulation associated with Kyle was not present (Fig. 10a). In addition, the CAD signature and CF were present, as with CTL (albeit not as strong). In fact, higher temperatures were observed in the ADR at initial conditions in NS due to a more easterly flow east of the ADR in the absence of Kyle (i.e. TC removal). Such flow advected the warmer air-mass inland at 10/10/00Z.

The cross-section revealed the CAD profile in the NC Piedmont with mean northeasterly winds and lower near-surface θ in the east side of the mountains (Fig. 10b). The temporal changes of the SLP, θ, and wind profiles were lesser than in CTL due to the TC removal. This is shown by the continuity of the CAD throughout this simulation. By 10/10/12Z the CAD signature had improved, with the baroclinic zone associated with the CF being accentuated (Fig. 10c). The continuity of the surface ridge over New England maintained a favorable flow regime that sustained the event, as colder air and northeasterly flow remained east of the mountains (Fig. 10d).

From 10/11/00Z onwards the CAD event was still present, though some erosion ensued as the ridge weakened and retreated northeastward (Fig. 11a). Meanwhile, the flow changed from the east-southeast while advecting the CF inland (similar than in CTL). The cross-section during this period confirmed that the front had moved inland into the NC Piedmont (Fig. 11b). The CAD signature reached its weakest point at 10/11/12Z (Fig. 11c), though it was still present in a limited swath along the Foothills, and the front became stationary (Fig. 11d). The ridge then began to retreat northeastward by 10/12/00Z, thus favoring CAD re-strengthening (Fig. 12a). In the vertical profile the CAD was still limited to the Foothills (Fig. 12b).

By the end of the period the CAD signature was still present with the ridge being the main driver of the surface patterns in the ADR (10/12/12Z; Fig. 12c). The CF had persisted (albeit weaker) throughout the simulation. This nearly-unchanged vertical environment was also reflected at the end of period by 10/12/12Z (Fig. 12d). The effects of turning off moisture fluxes in this case remain unclear, and future sensitivity tests may shed more light on the subject. However, the results presented herein reflect a remarkable similarity of all fields when compared to CTL, with the obvious exception of Kyle's removal. The results in case NS confirmed: 1) The removal of Kyle from the initial conditions, 2) The persistency of the CAD despite fluctuations in strength, and 3) The steady presence of the baroclinic zone associated with the CF. The CAD was modulated by changes in the strength and position of the ridge located to the northeast of the ADR.

5.2.3 ***FLAT simulation***

Kyle's track in case FLAT was similar than in CTL (Sec. 5.1), thus we will discuss on the other major changes in the weather patterns during this simulation (Figs. 13-15). The topography removal began its effects on the pre-existing CAD almost immediately. As the blocking was removed, the air-mass was able to flow westward through and away from the ADR, as confirmed by surface winds and uniformly cooler θ west of the region at 10/10/00Z (Fig. 13a). The colder θ remnants of the CAD were still evident in the vertical cross-section as the readjustment process was not instant (Fig. 13b). It was anticipated that the CAD event had to dissipate in its entirety within 24 hours of initialization. By 10/10/12Z all indicators of the CAD event had disappeared. The isobars flattened as the air flowed westward throughout the ADR with no blocking (Fig. 13c). Consistent with this observation, the vertical profile showed that the cold air-mass had redistributed westward in response to the predominant easterly-southeasterly flow in the ADR (Fig. 13d). These changes set the benchmark that for this case the CAD was absent, while the TC and CF were still present.

As Kyle approached the GA coast (10/11/00Z) the southeasterly flow began to strengthen along the NC-SC coastline while advecting the CF inland (Fig. 14a), a similar behavior to that in case CTL. The interaction between the southeasterly flow from the storm and the northeasterly winds from the ridge helped in the maintenance of the frontal boundary inland. The two air-masses were evident in the cross-section (Fig. 14b), with lower θ west of the boundary (note surface SE to NE wind direction change) and higher values immediately east of it. By 10/11/12Z the storm was nearing SC while advecting warmer temperatures well into the Piedmont region (Fig. 14c). The front was further inland during this timeframe as Kyle had eroded the presence of the ridge in the study area. This demarcation was more evident in the cross-section of Figure 14d, with the southeasterly flow of the warm sector extending west into the Piedmont, and northeasterly winds just to the west. Further west the southeasterly flow resumed along 35°N due to a more zonal orientation of the baroclinic zone as opposed to in case CTL. Evidently, the absence of the CAD played a role in this particular orientation of the CF and baroclinic zone. At 12/12/00Z Kyle was located in the NC-SC coastline while on ET transition (Fig. 15a), again similar to CTL. The front began to move eastward (as shown in cross-section) in response to the storm's influence (Fig. 15b). By 10/12/12Z the ET low was near Cape Hatteras and moving offshore (Fig.15c). The colder air-mass prevailed in most of the study region in the wake of the front (located offshore at that point), while the NC Outer Banks were still under the influence of the storm (Fig. 15d).

The results from the three cases herein discussed lead us to conclude that: 1) The simulated TC-CAD event in CTL was positively verified when compared against the observations, 2) Kyle was successfully removed from case NS, while the CAD event remained in place, and 3) The topography removal in case FLAT effectively ended the CAD event, while Kyle tracked mostly unaffected by these changes.

6. **Impacts of the Interaction of CAD and Kyle on Precipitation**

*6.1 **Precipitation***

Figure 16 shows the total accumulated precipitation for the entire simulation period in cases CTL, NS and FLAT, respectively. Additionally, the CPC Precipitation and ERA-I total accumulated rainfall were included. There were three observed swaths of accumulated precipitation that served as a metric to verify the simulated rainfall (Fig. 16a): 1) The main swath extending from north-central SC through central NC and widening from south-central VA to eastern NC, 2) The coastal swath of precipitation extending from north FL to Cape Hatteras with a peak in coastal SC, and 3) An external swath of precipitation extending from central Tennessee (TN) to Kentucky and West Virginia. The latter was unassociated with the TC-CAD event, but served as a metric for comparing the different simulation results. This particular swath existed in all three simulations with similar results (as shown in Figs. 16c, 16d, and 16e, respectively), extending from central TN towards northern VA, and it was associated with a surface low that combined with a shortwave mid to upper-level trough that approached the study area from the west (Figs. 18a and 18b). CTL results (Fig. 16c) also showed the three observed swaths of precipitation, albeit stronger in the coastal sections in response to a stronger simulated storm. However, a thin swath of precipitation along the east side of the NC Appalachians extending through central VA towards the DC area showed in this case. An examination of the model initialization data (Fig. 16b) revealed an inland bias of the ERA-I data that influenced to force the same bias in our CTL results. Such can be explained by an overrepresentation of the interaction between an impending 500 hPa trough vorticity maximum over western NC (see Fig. 18) and Kyle during 10/11. The same precipitation pattern occurred in FLAT (Fig. 16e), thus ruling out any major influence from the topography in that inland swath of precipitation. The precipitation area over the coast was directly caused by the storm as it tracked along the area during 10/11-10/12. Despite this, the relationship of the ongoing CAD event and Kyle in the main swath over the ADR was unclear. It needs to be mentioned that the rainfall accumulations in CTL underperformed both in location and intensity within the ADR. However, the results discussed above confirmed the validity of CTL from the context of sensitivity tests of CAD and TC removal in a CAD-TC environment.

In case NS, the total accumulated precipitation quantity and distribution departed dramatically from that in case CTL (Fig. 16d). As expected, coastal precipitation disappeared completely, but the most significant changes occurred in the other areas of precipitation originally present in the ADR and eastern NC (see CTL). No major accumulated precipitation occurred in the central and eastern Carolinas. A single swath of scattered light precipitation located in the western NC-SC Piedmont region into VA is attributed to the CAD itself. Otherwise, no major precipitation amounts fell in the study area in the absence of the storm, suggesting that the CAD may have not been responsible for the observed heavy amounts.

The above is verified by the simulated results of case FLAT, with the main accumulated precipitation areas similar than in CTL (Fig. 16e). Some differences can be seen in the rainfall accumulation of FLAT and CTL, which are attributed to the removal of the topography and the lack of orographic lifting, a favoring factor in precipitation generation. This is observed in the Appalachian swath of accumulated precipitation in FLAT, which was slightly stronger weaker in western NC. In addition it was displaced just to the east when compared to CTL due to a more eastern track of the simulated storm in the former.

It was found that CTL precipitation had good results within the scope of our study, thus serving as a benchmark for the sensitivity tests. Cases NS and FLAT had large discrepancies in terms of precipitation accumulation quantity and distribution. In NS, the absence of the storm reduced dramatically the accumulated precipitation, leaving only minor amounts of precipitation in the Piedmont and Foothills regions. Otherwise, no major precipitation was accumulated along the coast moving inland to the central parts of the area. It needs to be pointed out, however, that the deactivation of surface fluxes of heat and moisture might have played a role in the decreased rainfall accumulation in the ADR for this case. Despite this, the high amount of precipitation outside the ADR associated with the low west of the Appalachians, plus the different distribution of rainfall in this case suggests that the effects of these changes in the simulation were comparatively minor. On the other hand, FLAT results were quite similar to CTL in terms of quantity and distribution of accumulated precipitation. These sensitivity tests suggested that the bulk of the total accumulated precipitation was produced by the storm, and that the CAD event had minor impact on the amount of rainfall in this case.

6.2 ***Evolution of the coastal front (CF)***

The changes and behavior of the CF in the three simulations discussed in Section 5.2 led us to a closer examination to determine its influence in heavy precipitation in the study region. It was found that this surface feature was observed in all three simulations, while its position shifted from coast to inland sections during particular periods. The strong horizontal near-surface thermal gradient was forced by the land-sea contrast, with cooler values over the continent and the warmer SSTs associated with the Gulfstream (not shown). This gradient is the driver of its formation, while the weather pattern associated with the CAD, ridging, and later Kyle favored the observed changes in position and strength. With its influence and previously-discussed role in heavy precipitation during TC-CAD events (e.g. SB09), questions arose with respect of this case.

In CTL (Sec. 5.2.1) a CF signature was initially located near the GA-NC coastline and began to strengthen as Kyle approached the study region during 10/10. The outer circulation then began to push the CF inland, ending as far west as the NC Piedmont by 10/11. Afterwards, the front began to move eastward in response to Kyle's passage to the southeast of the ADR (10/12). For case NS (Sec. 5.2.2) the frontal characteristics were remarkably similar to those in CTL. Again, the front was located near the coast by 10/10 and moved inland by 10/11, later returning close to the coast by 10/12. However, due to the Kyle's absence, the main driver for the inland motion was the ridge that developed further south in this case. The ridge's influence was steadier, which in turn accounted for the slower (stationary at times) frontal motion. Its strength was also slightly weaker in this case, probably due to the lesser advection of warmer temperatures that was observed without Kyle. The frontal behavior in case FLAT (Sec. 5.2.3) was again similar to previous two cases. The circulation associated with Kyle was responsible for the warm-air advection that further strengthened the CF as it was also pushed inland into the Piedmont. In this case, however, there was no CAD present, which altered the frontal characteristics. For example, the orientation turned out to be more zonal due to the absence of the ageostrophic flow (e.g. stronger northeasterly winds in the ADR) associated with the CAD (B03).

An examination of the CF reveals that it was present throughout the study period for all three cases. This is a departure from the contrasting precipitation accumulations for the same cases, that is, the front was still present in the "dry" case NS. This fact leads us to conclude that while still affecting a local influence, the CF was not the major driver in heavy precipitation accumulated in the Carolinas during this particular event. Despite this, the CF may influence strongly in heavy precipitation when another source is present, Kyle in this case. This would not represent a contradiction with the findings in SB09, but much rather a highlighting of the crucial role of the storm's presence and direct interaction with a frontal boundary. Additionally, it is worth noting that the final influence of the CF in heavy precipitation for this case was not assessed, for it would require a new set of simulations comparing the changes in its absence, which is out of the scope of our study.

6.3 ***Role of Kyle in heavy precipitation***

In light of the little observed impact of the CAD absence on the final precipitation accumulations, it became clear that it had a minor role in the generation of heavy rain during this particular case. Consequentially, a blend of surface and mid-level fields during two selected periods (discussed below) showed that the bulk of heavy precipitation was caused by Kyle as it moved over the NC-SC coastline. Figure 17 shows an overlay of 10-m wind barbs, 950 hPa equivalent potential temperature (θ_e), 850 hPa reflectivity (DBZ), and 700 hPa vertical moisture flux for all cases in the periods of 10/11/12Z and 10/12/00Z, respectively. Figure 18 contains 500 hPa relative vorticity, winds and geopotential height in the same cases and period as those in Fig. 17.

In CTL, by 10/11/12Z Kyle's circulation was affecting the entire study region, while two distinct DBZ areas were observed (Fig. 17a): one in the SC-NC coastline and another in the western Piedmont and mountains. Higher θ_e concentrated along the coastal section as it was advected by Kyle into the eastern sections of NC and SC. The positive θ_e advection in the lower levels increased the extent to which θ_e decreases with height (e.g. a more negative $d\theta_e/dz$) thus favoring an increase of potential instability. This destabilization associated with the storm in CTL would eventually trigger the development of deep convective precipitation, as pointed out by Markowski and Richardson (2012). In addition, there was a positive correlation of these areas of precipitation with areas of vertical moisture flux. The latter is defined as $q_v w$ (Lin 2007), where q_v and w are the water vapor mixing ratio and vertical motion, respectively. It is considered as one of the common ingredients for heavy orographic precipitation (Lin et al. 2001). However, only low values (~ 0.1 x 10^{-3} m s^{-1}) were occurring, thus indicating that the precipitation was mostly light to moderate at this point. In the mid-levels the pattern was dominated by a 500 hPa trough west of the study region, the vorticity maximum (hereafter VORTMAX) associated with Kyle located over coastal SC and a ridge to the east of the storm (Fig. 18a). The isopleths and wind barbs confirmed that a positive vorticity advection (PVA) maximum was about to reach eastern NC by this point. The sources were Kyle and the impending trough to the west. Consistently, the pattern evolved significantly by 10/12/00Z when Kyle was located over eastern SC-NC, and heavy precipitation had developed and concentrated over eastern NC and southeast VA (SE-VA hereafter; Fig. 17b). At the same time peak θ_e (>338 K) clustered over eastern NC and SE-VA, in good correlation with the highest DBZs. Additionally, the strengthening cold front could be observed in tandem with the transitioning cyclone where the strongest temperature gradient was located. Increased vertical moisture flux in Fig. 17b (~ 0.9 x 10^{-3} m s^{-1}) confirmed the conductive environment for heavy precipitation in the aforementioned region during this timeframe. The VORTMAX located in eastern NC/SE-VA was the main source for heavy precipitation in the area (Fig. 18b).

Perhaps the most revealing aspect for us was the absence of the VORTMAX associated with Kyle in NS while coinciding with little to no precipitation in the areas that observationally registered the highest amounts of precipitation. For example, in this case there was no coastal precipitation area at 10/11/12Z, but still there was an inland area of precipitation associated with the approaching trough (Fig. 17c). The highest θ_e also concentrated in the coastal and eastern Piedmont, though slightly lower than in case CTL. The aforementioned absence of a VORTMAX from Kyle was seen in the mid-levels (Fig. 18c) where the trough VORTMAX was present over the Mountains and approaching the Piedmont, as in CTL. By 10/12/00Z the departure of the results in case NS was most contrasting, with a small area of small DBZs (< 15 dBZ) occurring offshore NC Outer Banks and over extreme SE-VA (Fig. 17d). Again, the vertical moisture flux was minimum during this period, owing to the absence of any significant vertical forcing necessary for deep convective development. A more stable lower tropospheric environment was also present in this simulation, as evidenced by the lower θ_e. Despite the mid-level VORTMAX passage over the area (Fig. 18d), its lesser intensity, plus the absence of the destabilization and forcing brought by Kyle are counted as the main factors in the major reduction in accumulated precipitation in case NS. The existence of the CAD in combination with the CF and mid-level trough were not enough to generate heavy precipitation, the transitioning TC was the key ingredient.

To further corroborate these results, the 10/11/12Z precipitation distribution in case FLAT (Fig. 17e) had a remarkable similarity to the results in CTL consisting of the inland and coastal areas of precipitation, respectively. Vertical moisture flux was again occurring, but only modestly supporting convective development, and θ_e was increasing in coastal NC-SC in association to

Kyle. Most importantly, the VORTMAX associated with the storm was in this simulation (Fig. 18e), while the environmental mid-level conditions were otherwise very similar in all three cases. Later, precipitation increased along eastern NC and SE-VA by 10/12/00Z (Fig. 17f), with high DBZs (heavy precipitation) in those areas. Vertical moisture flux increased to similar or even greater values than those at the same time in CTL. The high values confirm that the forcing necessary for deep convection was again present in this simulation. The magnitude and distribution of θ_e in case FLAT were identical to CTL, owing to the destabilization impinged by the storm's presence. Again, the VORTMAX moved over eastern NC and SE-VA covering a broader region (Fig. 18f), thus generating more lifting in a larger area, which in turn resulted in a more widespread distribution of heavy precipitation.

In summary, an examination of near-surface and mid-level fields revealed that: 1) Kyle was the main driver of heavy precipitation in the study area, 2) An additional supply of mid-level vorticity brought by the storm merged with the maximum associated with an approaching trough, thus combining to generate heavy precipitation in the eastern side of our study region, 3) Kyle brought a destabilization of the lower troposphere that further enhanced the potential for heavy precipitation, and 4) A pre-existing CAD seemed to have little influence in the generation of heavy precipitation for this case. Regarding the CF, however, the results suggest that this feature did not have much influence on the precipitation generation when Kyle was absent. Despite this observation, an enhancing role of the CF in heavy precipitation for this case cannot be discarded.

7. **Summary**

A numerical case study of the interaction of Tropical Storm Kyle (2002) with an ongoing CAD event while passing near the ADR was done in order to assess the role of both systems in heavy precipitation in the Carolinas. Three cases were run using WRF-ARW: 1) CTL, a simulation approximating the observed conditions in the 10/10-10/12/2002 period, 2) NS, same as CTL but with Kyle removed from the initial conditions, and 3) FLAT, same as CTL but with topography removed in order to eliminate the CAD event. Two reanalysis datasets helped in positively verifying the simulated results in CTL. A CAD was present at initial conditions while Kyle was a tropical depression near the Bahamas. The storm then tracked towards the GA-NC coastline and interacted with the CAD and a frontal system as it recurved (in response to an approaching mid to upper-tropospheric trough) and began ET transition. Heavy precipitation associated with the event concentrated in three main corridors: 1) Along the GA to NC coastline, 2) Across central SC to the Albemarle Sound of NC, and 3) Inland along the Appalachian Mountains from western NC towards central VA. It was found that the pre-existing CAD was weakened and eventually dissipated by the storm's circulation as it tracked along the Carolina coastline. This is consistent with mechanism (iv) in Chapter 8.3.2 of Lackmann (2011): the passage of a coastal cyclone east of the ADR. The mechanism was the shift of the mean near-surface flow from the north and northwest associated to the circulation in the ADR, which directed the air mass away from the mountains in the ADR while effectively terminating the CAD. In addition, the increase of wind speeds in the region was another contributor to a reduction of the mountain blocking effect.

Contrasting results in accumulated precipitation led us to make an assessment on the role of the TC-CAD interactions in heavy precipitation occurrence. For example, the accumulated precipitations were similar in CTL and FLAT, but strikingly different in NS. In fact, the storm track, accumulated rainfall distribution and quantities in FLAT followed very similarly to the results in CTL. When Kyle was removed from the initial conditions (NS), the absence of a mid-level VORTMAX appeared to have been a major cause for the little accumulations in that simulation. In CTL and FLAT the respective VORTMAXs from Kyle and the approaching mid-level trough merged in eastern NC and SE-VA to generate the high precipitation accumulations in the region. The increase of 500 hPa relative vorticity and its favoring of positive low and mid-level vertical motion in the area represented an enhancement of two important ingredients for heavy precipitation: convergence and vertical moisture flux. In addition, Kyle brought an increasingly unstable layer to the area (e.g. higher θ_e) that further enhanced the rain event. The high degree of correlation of cases CTL and FLAT showed that a CAD event in the ADR had little impact in heavy precipitation associated with Kyle. Furthermore, case NS confirmed that the absence of the storm was the key element in rainfall generation. No forcing for heavy precipitation occurred due to the lack of advection and merging of Kyle' VORTMAX in the area. All of this despite the existence of the mid-level trough and associated VORTMAX ~~that~~ had moved over the study area during the same period. Thus, it appears that for this specific type of coastal track, the existence or not of a CAD event was not essential in the formation of heavy precipitation, but much rather the aforementioned ingredients: the storm and its associated forcing in combination with a favorable mid to upper-level environment.

SB09 concluded that the CF was crucial in the total accumulated precipitation during Tropical Storm Marcos (1990) via the forcing of ascending air along the boundary as the storm advected moist air from the southeast. In our case the CF was also present in tandem with the CAD event in observations and all simulations, as well. However, the CF alone was unable to force enough precipitation in NS due to the much lesser moist southeasterly flow brought by Kyle in the other two simulations (Fig. 16b). Since the CF was present in all cases, it is difficult to quantify its definite role in heavy precipitation generation for this case study. Despite this, it could be concluded than the CAD event was not responsible for any major precipitation event, or the maintenance of the CF itself, since the latter did persist throughout FLAT. SB09 recognized the complexity of their case study (e.g. multiple weather systems interacting simultaneously), thus making ours as a good complement to the subject, since we had a simpler setup. The ability to separately remove the two main weather systems of focus (Kyle and CAD) led us to these conclusions. Our results agree with those in SB09 in the aspect of the possible role of the combination between the CF and the instability brought by the storm.

The results above led us to conclude that the CAD was not influential on the development of heavy rain along the ADR and coastal Carolinas during Kyle's near passage. Instead, the role of the storm was determinant on the heavy precipitation amounts in this region. Contributing factors, such as, the major increase of mid-level relative vorticity, advection of moisture and increase of instability brought by the storm as it evolved into an ET cyclone are instead proposed to be the main drivers of heavy precipitation in this case. It appears that the fact that Kyle was in ET transition was also influential in the amount of precipitation accumulated in our study area.

The results presented here are evidence that further research needs to be done on the subject of TC-CAD interactions. Additional studies of past cases with both similar and different tracks and intensities are suggested as future framework. The use of all available tools, such as, observational data and numerical modeling to assess the effects of more TC-CAD cases can be of great help to operational forecasters in the ADR and coastal region at the time of issuing warnings to protect life and property in the area during future events.

Acknowledgments: The authors would like to acknowledge Barrett Smith and Jonathan Blaes at the National Weather Service office in Raleigh, NC, for their insights and ideas on the topic presented in this paper. The comments from three anonymous reviewers are highly appreciated, which helped improving the quality of the paper. We are also grateful to Dr. John Hemphill's review of the manuscript. This research was supported by the National Science Foundation Awards AGS-1265783, HRD-1036563, CNS-1126543, and CNS-1429464.

References

Bailey CM, Hartfield G, Lackmann GM, Keeter K, Sharp S (2003; B03) An Objective Climatology, Classification Scheme, and Assessment of Sensible Weather Impacts for Appalachian Cold-Air Damming. Weather and Forecasting 18:641-661

Bell GD, Bosart LF (1988) Appalachian Cold-Air Damming. Mon Wea Rev 116:137-161

Dee DP, Uppala SM, Simmons AJ, Berrisford P, Poli P, Kobayashi S, Andrae U, Balmaseda MA, Balsamo G, Bauer P, Bechtold P, Beljaars ACM, van de Berg L, Bidlot J, Bormann N, Delsol C, Dragani R, Fuentes M, Geer AJ, Haimberger L, Healy SB, Hersbach H, H´olm EV, Isaksen L, K°allberg P, K¨ohler M, Matricardi M, McNally AP, Monge-Sanz BM, Morcrette JJ, Park BK, Peubey C, de Rosnay P, Tavolato C, Th´epaut JN, Vitart F (2011) The ERA-Interim reanalysis: Configuration and performance of the data assimilation system. Quart J R Meteorol Soc 137:553-597. doi: 10.1002/qj.828

Forbes GS, Anthes RA, Thomson DW (1987) Synoptic and Mesoscale Aspects of an Appalachian Ice Storm Associated with Cold-Air Damming. Mon Wea Rev 115:564-591

Fredrick S, Davis C, Gill D, Low-Nam S (2009) Bogussing of tropical cyclones in WRF version 3.1. Technical report. National Center for Atmospheric Research, Boulder, Colorado, 6 pp.

Hong SY, Lim JOJ (2006) The WRF Single-Moment 6-Class Microphysics Scheme (WSM6). J Korean Meteor Soc 42:129-151

Hong SY, Noh Y, Dudhia J (2006) A New Vertical Diffusion Package with an Explicit Treatment of Entrainment Processes. Mon Wea Rev 134:2318-2341

Lackmann G (2011) Midlatitude Synoptic Meteorology: dynamics analysis, and forecasting. American Meteorological Society, Boston

Lin YL (2007) Mesoscale Dynamics. Cambridge University Press, Cambridge

Lin YL, Chiao S, Wang TA, Kaplan ML (2001) Some common ingredients for heavy orographic rainfall. Weather and Forecasting 16:633-660

Markowski P, Richardson Y (2012) Mesoscale Meteorology in Midlatitudes. Wiley-Blackwell, Hoboken

Mesinger F, DiMego G, Kalnay E, Mitchell K, Shafran PC, Ebisuzaki W, Jovic D, Woollen J, Rogers E, Berbery EH (2006) North American regional reanalysis. Bull Amer Meteor Soc 87:343-360

Mlawer EJ, Taubman SJ, Brown PD, Iacono MJ, Clough SA (1997) Radiative transfer for inhomogeneous atmospheres: RRTM, a validated correlated-k model for the longwave. J Geophys Res 102:16663–16682

Richwein BA (1980) The damming effect of the southern Appalachians. Natl Wea Dig 5:2-12

Skamarock WC, Klemp JB, Dudhia J, Gill DO, Barker DM, Duda M, Huang XY, Wang W, Powers JG (2008) A Description of the Advanced Research WRF Version 3. NCAR Technical Note, NCAR/TN-475 ? STR

Smith B, Blaes J, Garcia-Rivera J, Dale J (2013) A Climatology of Warm Season Cold-air damming and Tropical Cyclones in the Southeast U.S. Preprints, 38th Annual Meeting, North Charleston, SC, National Weather Association, P1.11

Srock AF, Bosart LF (2009) Heavy Precipitation Associated with Southern Appalachian Cold-Air Damming and Carolina Coastal Frontogenesis in Advance of Weak Landfalling Tropical Storm Marco (1990). Mon Wea Re 137:2448-2470

Stauffer DR, Warner TT (1987) A Numerical Study of Appalachian Cold-Air Damming and Coastal Frontogenesis. Mon Wea Re 115:799-821

Stewart S (2002) Hurricane Kyle Tropical Cyclone Report. National Hurricane Center, Miami, FL. http://www.nhc.noaa.gov/data/tcr/AL122002_Kyle.pdf. Accessed 30 April 2015

WPC Surface Analysis Archive (2014a). Weather Prediction Center. http://www.wpc.ncep.noaa.gov/archives/web_pages/sfc/sfc_archive.php. Accessed 15 June 2014

WPC Tropical Storm Kyle, October 9-12, 2002 (2014b) http://www.wpc.ncep.noaa.gov/tropical/rain/kyle2002rainfilledwhite.gif. Accessed 15 June 2015

Xiao Q, Zou X, Wang B (2000) Initialization and simulation of a landfalling hurricane using a variational bogus data assimilation scheme. Mon Wea Rev 128:2252-2269

Xiao Q, Chen L, Zhang X (2009) Evaluations of BDA Scheme Using the Advanced Research WRF (ARW) Model. J Appl Meteor Climatol 48:680-689

Xu Q (1990) A Theoretical Study of Cold-Air Damming. J Atmos Sci 47:2969-2985

Xu Q, Gao S (1995) An Analytical Model of Cold-air damming and Its Applications. J Atmos Sci 52:353-366

Table captions

Table 1: Features of the three cases used to isolate the effects of CAD and Kyle.

Table 2: List of abbreviations.

Table 1: Features of the three cases used to isolate the effects of CAD and Kyle.

Table 2: List of abbreviations.

ADR	Appalachian Damming Region
B03	Bailey et al. (2003)
CAD	Cold-air damming
CF	Coastal front
CPC	Climate Prediction Center
CTL	Control case
DBZ	Reflectivity
DC	District of Columbia
ERA-I	ERA-Interim global reanalysis dataset
ET	Extra-tropical transition
FLAT	No-mountain case
GA	Georgia
NARR	North American Regional Reanalysis
NC	North Carolina
NE	Northeast
NHC	National Hurricane Center
NS	No-storm case
PVA	Positive vorticity advection
SB09	Srock and Bosart (2009)
SC	South Carolina
SE	Southeast

SLP	Sea level pressure
SST	Sea surface temperature
TC	Tropical Cyclone
TN	Tennessee
VA	Virginia
VORTMAX	Vorticity maximum
WRF-ARW	Weather Research and Forecast Model – Advanced Research WRF

Figure Captions

Figure 1: ERA-I sea-level pressure contours (mb) 10-m wind barbs and 2-m temperature (shaded, in degrees Kelvin) in a 12-h intervals from 10/10/00Z to 10/11/12Z. The “x” denotes the center location based on NHC best track data for the respective plot times.

Figure 2: As in Fig. 1, but for 10/12/00Z (left panel) to 10/12/12Z (right panel).

Figure 3: NARR sea-level pressure contours (mb) 10-m wind barbs and 2-m potential temperature (shaded, in degrees Kelvin) in 12-h intervals from 10/10/00Z to 10/10/12Z (left panels), and 12-h total accumulated precipitation (shaded, in mm) and convective precipitation (contours, in mm) for the same respective periods (right panels). The “x” denotes the center location based on NHC best track data for the respective plot times.

Figure 4: As in Fig. 3, but for 10/11/00Z (top panels) and 10/11/12Z (bottom panels).

Figure 5: As in Fig. 3, but for 10/12/00Z (top panels) and 10/12/12Z (bottom panels).

Figure 6: Simulated (filled circles) versus observed (open squares) tracks for CTL (a) and FLAT (b) simulations during the period from 0000 UTC 10 October 2002 to 1200 UTC 12 October 2002. Observed track data obtained from the National Hurricane Center "best track”. Three geographic regions of interest are also labeled on (a).

Figure 7: CTL-simulated sea-level pressure contours (mb) 10-m wind barbs and 2-m potential temperature (shaded, in degrees Kelvin) in 12-h intervals from 10/10/00Z to 10/10/12Z (left panels), and vertical cross-sections (taken along 35°N) of potential temperature (shaded, in degrees Kelvin) and horizontal wind barbs across the Appalachian Mountains eastward to the NC Outer Banks (denoted as OBX) for the same respective periods (right panels). The red line in the left panels represent the segment depicted in the cross-sections on the right.

Figure 8: As in Fig. 7, but for 10/11/00Z (top panels) and 10/11/12Z (bottom panels).

Figure 9: As in Fig. 7, but for 10/12/00Z (top panels) and 10/12/12Z (bottom panels).

Figure 10: As in Fig. 7, but for case NS for 10/10/00Z (top panels) and 10/10/12Z (bottom panels).

Figure 11: As in Fig. 7, but for case NS for 10/11/00Z (top panels) and 10/11/12Z (bottom panels).

Figure 12: As in Fig. 7, but for case NS for 10/12/00Z (top panels) and 10/12/12Z (bottom panels).

Figure 13: As in Fig. 7, but for case FLAT for 10/10/00Z (top panels) and 10/10/12Z (bottom panels).

Figure 14: As in Fig. 7, but for case FLAT for 10/11/00Z (top panels) and 10/11/12Z (bottom panels).

Figure 15: As in Fig. 7, but for case FLAT for 10/12/00Z (top panels) and 10/12/12Z (bottom panels).

Figure 16: Total accumulated precipitation (mm) for CPC Precipitation (a), ERA-I (b) CTL (c), NS (d) and FLAT (e) during each entire period: 10/10/00Z to 10/13/00Z.

Figure 17: Simulated 900 hPa equivalent potential temperature (red contours, in degrees Kelvin), 850 hPa reflectivity (shaded, in dBZ), 700 hPa vertical moisture flux (black contours, in intervals from 0.1 to 0.9 x 10-3 m s-1), and 10-m wind barbs for cases: CTL (top panels), NS (middle panels) and FLAT (bottom panels), during 10/11/12Z (left panels) and 10/12/00Z (right panels).

Figure 18: Simulated 500 hPa relative vorticity (shaded, in 10-5 s-1), geopotential height (contours, in m), and wind barbs for cases: CTL (top panels), NS (middle panels) and FLAT (bottom panels), during 10/11/12Z (left panels) and 10/12/00Z (right panels).

Figure 1: ERA-I sea-level pressure contours (mb) 10-m wind barbs and 2-m temperature (shaded, in degrees Kelvin) in 12-h intervals from 10/10/00Z to 10/11/12Z. The “x” denotes the center location based on NHC best track data for the respective plot times.

Figure 2: As in Fig. 1, but for 10/12/00Z (left panel) to 10/12/12Z (right panel).

Figure 3: NARR sea-level pressure contours (hPa) 10-m wind barbs and 2-m potential temperature (shaded, in degrees Kelvin) in 12-h intervals from 10/10/00Z to 10/10/12Z (left panels), and 12-h total accumulated precipitation (shaded, in mm) and convective precipitation (contours, in mm) for the same respective periods (right panels). The “x” in the left panels denote the center location based on NHC best track data for the respective plot times.

Figure 4: As in Fig. 3, but for 10/11/00Z (top panels) and 10/11/12Z (bottom panels).

Figure 5: As in Fig. 3, but for 10/12/00Z (top panels) and 10/12/12Z (bottom panels).

Figure 6: Simulated (filled circles) versus observed (open squares) tracks for CTL (a) and FLAT (b) simulations during the period from 0000 UTC 10 October 2002 to 1200 UTC 12 October 2002. Observed track data obtained from the National Hurricane Center "best track”. Three geographic regions of interest are also labeled on (a).

Figure 7: CTL-simulated sea-level pressure contours (hPa) 10-m wind barbs and 2-m potential temperature (shaded, in degrees Kelvin) in 12-h intervals from 10/10/00Z to 10/10/12Z (left panels), and vertical cross-sections (taken along 35°N) of potential temperature (shaded, in degrees Kelvin) and horizontal wind barbs across the Appalachian Mountains eastward to the NC Outer Banks (denoted as OBX) for the same respective periods (right panels). The red line in the left panels represent the segment depicted in the cross-sections on the right.

Figure 8: As in Fig. 7, but for 10/11/00Z (top panels) and 10/11/12Z (bottom panels).

Figure 9: As in Fig. 7, but for 10/12/00Z (top panels) and 10/12/12Z (bottom panels).

Figure 10: As in Fig. 7, but for case NS for 10/10/00Z (top panels) and 10/10/12Z (bottom panels).

Figure 11: As in Fig. 7, but for case NS for 10/11/00Z (top panels) and 10/11/12Z (bottom panels).

Figure 12: As in Fig. 7, but for case NS for 10/12/00Z (top panels) and 10/12/12Z (bottom panels).

Figure 13: As in Fig. 7, but for case FLAT for 10/10/00Z (top panels) and 10/10/12Z (bottom panels).

Figure 14: As in Fig. 7, but for case FLAT for 10/11/00Z (top panels) and 10/11/12Z (bottom panels).

Figure 15: As in Fig. 7, but for case FLAT for 10/12/00Z (top panels) and 10/12/12Z (bottom panels).

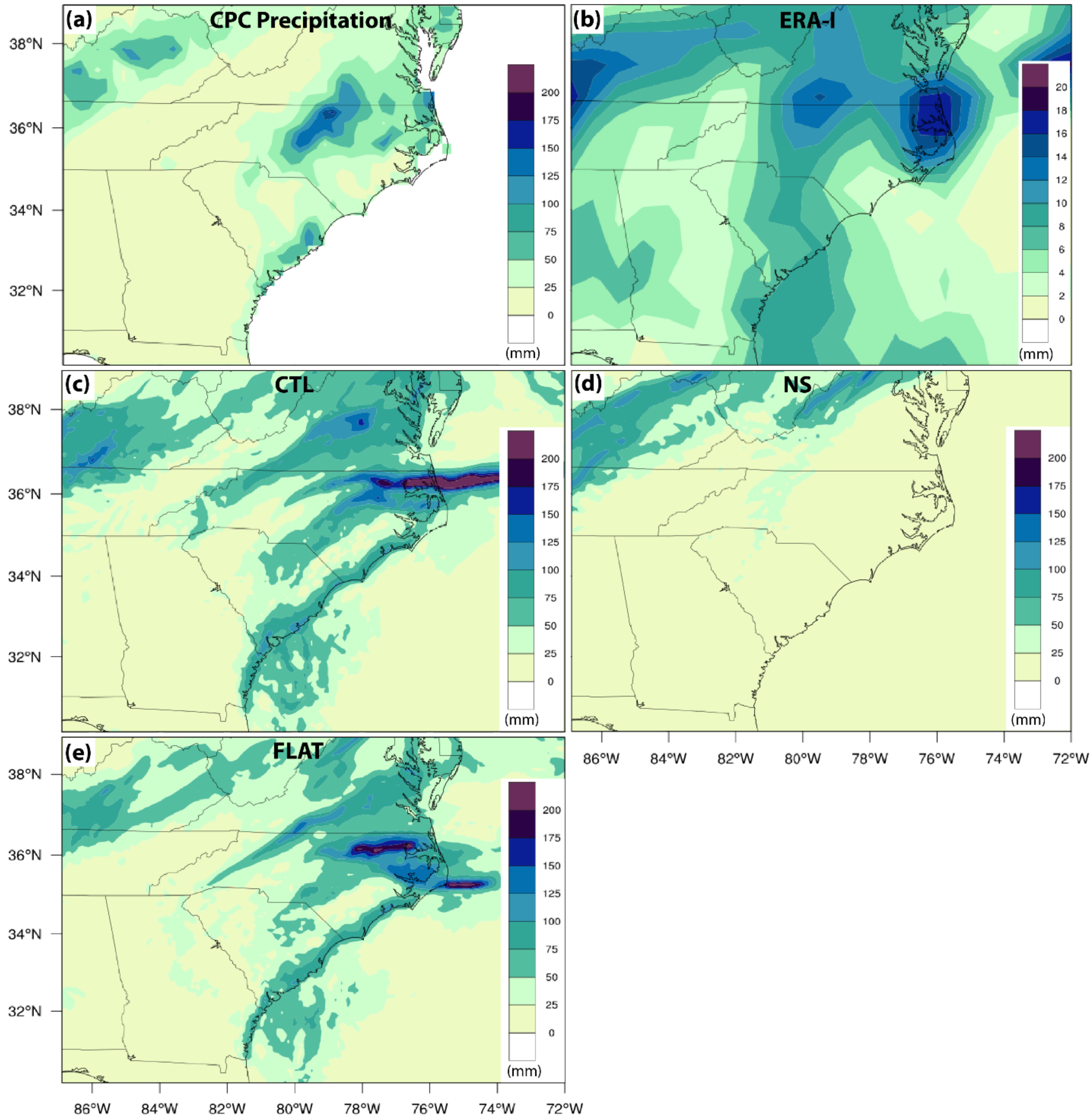

Figure 16: Total accumulated precipitation (mm) for CPC Precipitation (a), ERA-I (b) CTL (c), NS (d) and FLAT (e) during each entire period: 10/10/00Z to 10/13/00Z.

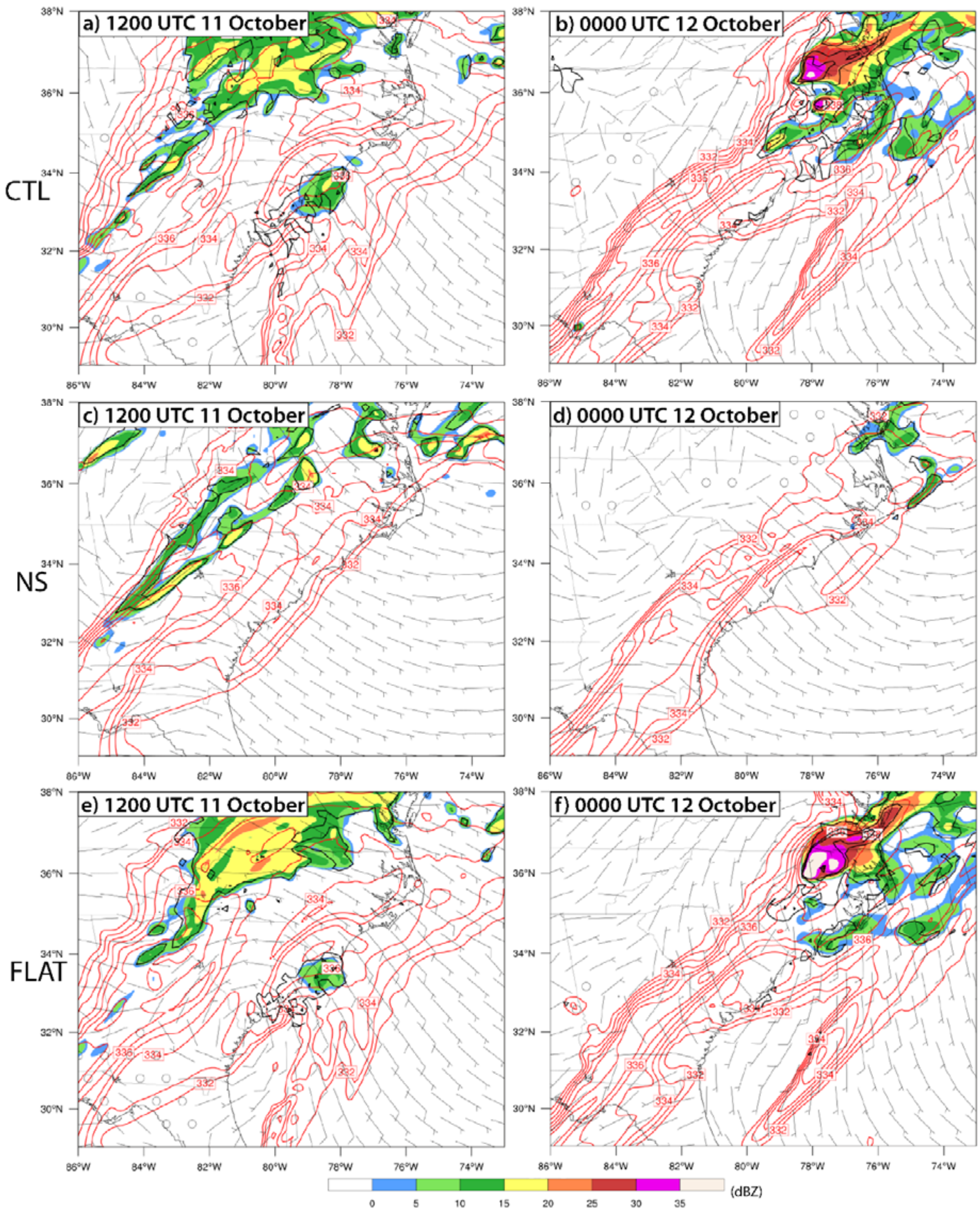

Figure 17: Simulated 900 hPa equivalent potential temperature (red contours, in degrees Kelvin), 850 hPa reflectivity (shaded, in dBZ), 700 hPa vertical moisture flux (black contours, in intervals from 0.1 to 0.9 x 10-3 m s-1), and 10-m wind barbs for cases: CTL (top panels), NS (middle panels) and FLAT (bottom panels), during 10/11/12Z (left panels) and 10/12/00Z (right panels).

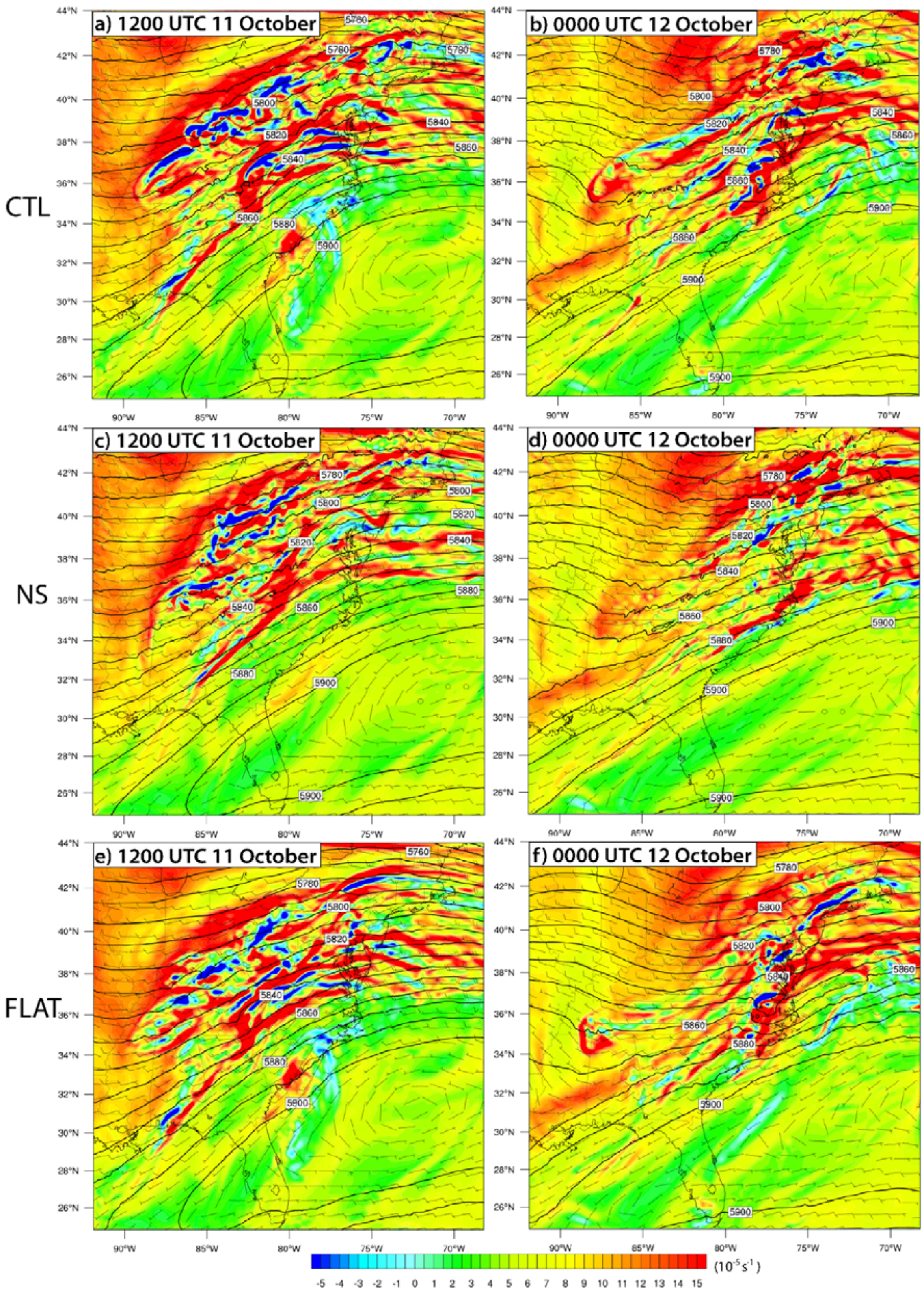

Figure 18: Simulated 500 hPa relative vorticity (shaded, in 10^{-5} s^{-1}), geopotential height (contours, in m), and wind barbs for cases: CTL (top panels), NS (middle panels) and FLAT (bottom panels), during 10/11/12Z (left panels) and 10/12/00Z (right panels).